

Structure-Based Design of a Eukaryote-Selective Antiprotozoal Fluorinated Aminoglycoside

Hiroki Kanazawa^[a], Oscar M. Saavedra,^[b] Juan Pablo Maianti,^[b] Simon A. Young,^[c] Luis Izquierdo,^[d] Terry K. Smith,^{*[c]} Stephen Hanessian,^{*[b]}, Jiro Kondo^{*[a,e]}

[a] *Dr. H. Kanazawa. Dr. J. Kondo*

Graduate School of Science and Technology, Sophia University, 7-1 Kioi-cho, Chiyoda-ku, 102-8554 Tokyo (Japan)

E-mail: j.kondo@sophia.ac.jp

[b] *Dr. O. M. Saavedra, Dr. J. P. Maianti, Prof. S. Hanessian*

Department of Chemistry, Université de Montréal, C.P. 6128, Succursale Centre-Ville, Montréal, Québec H3C 3J7 (Canada)

E-mail : stephen.hanessian@umontreal.ca

[c] *Dr. S. A. Young, Prof. T. K. Smith*

Biomedical Sciences Research Complex, University of St. Andrews, St. Andrews, Fife, Scotland KY16 9ST (United Kingdom)

E-mail : tks1@st-andrews.ac.uk

[d] *Dr. L. Izquierdo*

ISGlobal, Hospital-Clinic-Universitat de Barcelona, Barcelona (Spain)

[e] *Dr. J. Kondo*

Department of Materials and Life Sciences, Faculty of Science and Technology, Sophia University, 7-1 Kioi-cho, Chiyoda-ku, 102-8554 Tokyo (Japan)

- Aminoglycosides (AG) are antibiotics that lower the accuracy of protein synthesis by targeting a highly-conserved RNA helix of the ribosomal A-site. The discovery of AGs that selectively target the eukaryotic ribosome, but lack activity in prokaryotes, are promising as antiprotozoals for the treatment of neglected tropical diseases, and as therapies to read-through point-mutation genetic diseases. However, a single nucleobase change A1408G in the eukaryotic A-site leads to negligible affinity for most AGs. Herein we report the synthesis of 6'-fluoro sisomicin, the first 6'-fluorinated aminoglycoside, which, selectively interacts with the protozoal cytoplasmic rRNA A-site, but not the bacterial cytoplasmic A-site based on the respective X-ray co-crystal structures. The disposition 6'-F sisomicin within the bacterial and protozoal A-sites respectively reveal that fluorine acts only as an H-bond acceptor to favorably interact with G1408 of the protozoal A-site. Unlike aminoglycosides containing a 6'-amino group, 6'-F sisomicin cannot form a pseudo pair with A1408 of the bacterial A-site, which usually also benefits from additional hydrogen bonds. Based upon these structural observations it may be possible to shift the antibacterial activity of classical aminoglycosides to act preferentially as antiprotozoals. These findings expand the repertoire of small-molecules targeting the eukaryotic ribosome and demonstrate the usefulness of fluorine as a design element.

Introduction

Aminoglycosides composed of two to four sugar rings with positively charged ammonium groups anchored on a deoxystreptamine core are among the major classes of marketed antibiotics used worldwide for more than half a century.^[1,2] The aminoglycosides target an RNA molecular switch in the bacterial ribosomal tRNA acceptor site (A-site) and disrupt the fidelity of the decoding process in translation.^[3] The binding modes of aminoglycosides such as paromomycin, geneticin (G418) and sisomicin within the double-stranded RNA helix of the bacterial A-site have been extensively investigated at the atomic level by X-ray analysis.^[4-6] Relying on extensive structural information, collaborative efforts by our research groups have focused on the design and semi-synthesis of several aminoglycoside analogs intended to improve antibacterial activity and minimize toxicity to mammals.^[7-13] Among the sugar rings present in aminoglycosides, ring I plays the most important role in the binding specificity to the ribosomal A-site in bacteria, owing to its deep placement within the double-stranded RNA and the internal loop, where it participates in a stable pseudo base-pair interaction through two hydrogen bonds with the nucleobase A1408 (*E. coli* ribosomal RNA numbering).^[4-6] The rRNA sequence of the bacterial and protozoal A-sites are identical with the exception of A1408 that is replaced by a guanosine in the protozoal cytoplasmic ribosomal A-site.(Figure 1)^[4-6,14] Interestingly, bacteria can develop ribosomes that are resistant to multiple aminoglycoside classes, whereby the pseudo base-pair is altered by mutating the adenine nucleobase A1408 to a guanine in the chromosomal

16S rRNA loci,^[14] or by enzymatic methylation to *N*1-methyl-adenine.^[15] Other prevalent mechanisms of bacterial resistance also target the common ring I of aminoglycosides, such as enzymatic *O*-phosphorylation of the 3'-hydroxyl group, thus abrogating the specific interactions with A1408.^[16]

Although aminoglycosides are generally known for their antibacterial activity, they have valuable attributes that can be used against some important protozoal and fungal infections.^[17] In fact, the naturally occurring aminoglycoside paromomycin is a widely used antiprotozoal agent in India.^[18,19] Since eukaryotes commonly possess a guanine nucleobase at the 1408 position of the cytoplasmic ribosomal RNA (*E. coli* ribosomal RNA numbering), only a few aminoglycoside antibiotics containing an 6'-OH in ring I, such as geneticin (G418) and paromomycin, can bind to the eukaryotic ribosomal A-sites,^[14,17,20] while other aminoglycosides such as neomycin with a 6'-NH₃⁺ group, for example, cannot (Figure 1). Based upon these structural observations, we recently reported the synthesis of 6'-OH sisomicin, where the 6'-amino group was replaced by a hydroxyl (Figure 2).^[21] X-Ray analysis of this compound in complex with the protozoal A-site reveals a pseudo base-pair with G1408 through two hydrogen bonds and one C-H...O interaction.(Figure 2) As a consequence, the 6'-OH behaves as the acceptor of a hydrogen bond as exemplified by an O6'...H-N2_{G1408} interaction (Figure 3).²¹ Moreover, we corroborated that 6'-OH sisomicin exhibited antiprotozoal activity against several pathogenic species.^[21] On the other hand, an aminoglycoside with a 6'-NH₃⁺ in ring I cannot participate in a pseudo base-pair with G1408, because the NH₃⁺ group can only behave as

a hydrogen bond donor (Figure 3). In 1978, Mallams and coworkers^[22] isolated 6'-OH sisomicin as a minor hydrolysis byproduct from a naturally occurring dimeric aminoglycoside named 66-40C.^[22,23] Biological testing revealed that 6'-OH sisomicin had reduced antibacterial activity compared to sisomicin. However, 6'-OH sisomicin did show improved antibiotic potency against a resistant strain of *E. coli* carrying an AAC(6') enzyme isoform. This was not unexpected since this enzyme is involved in the acetylation of the 6'-NH₃⁺ group in sisomicin and related aminoglycosides which is now replaced by a 6''-hydroxyl group. It is of interest in the context of the work presented herein, that 6'-OH sisomicin exhibited antiprotozoal activity against *Trichomonas vaginalis*, *Entamoeba histolytica* (JH strain) comparable to paromomycin, which suggested that the sisomicin scaffold is a good starting point for the design of antiprotozoal aminoglycosides.^[21,22]

The translation accuracy of the human cytoplasmic ribosome is also diminished by aminoglycosides that bind the eukaryotic A-site, which has promising applications for the treatment of rare genetic diseases caused by single point mutations that functionally ablate a protein.^[24-28] For example, aminoglycoside-induced translational read-through of a premature STOP codon in the Cystic Fibrosis Transmembrane Conductance Regulator (CFTR) gene is thought to allow a portion of the truncated protein to reach its functional mature state.^[24-28]

In view of the potential emergence of resistant ribosome variants in bacterial strains, the need for anti-parasitic medications, and a multitude of biomedical applications, the discovery of a new generation of semi-synthetic

aminoglycosides that could selectively target ribosomal A-sites harboring a G1408 nucleobase would be of particular interest.

In the present study, we have designed and synthesized a sisomicin derivative with a fluorine atom at the 6' position instead of the 6'-amino group based on the assumption that the fluorine atom in 6'-F sisomicin would behave only as the acceptor of a hydrogen bond and interact favorably with G1408 in the cytoplasmic A-site of protozoa. In a previous study, we observed an F...H-N hydrogen bond interaction between a fluoro-amino N-acyl appendage on the deoxystreptamine core unit of a neomycin analog within the bacterial A-site, in which the F atom behaved as the hydrogen-bond acceptor.^[13] Therefore, we hypothesized that 6'-F sisomicin would preferentially interact with G1408 of the protozoal cytoplasmic rRNA A-site and not with A1408 in the bacterial A-site. In order to obtain comparative data, we carried out the X-ray analyses of 6'-F sisomicin bound to both the bacterial and protozoal cytoplasmic rRNA A-sites to demonstrate which variant results in more effective interactions. This property in turn would augur well for the development of a eukaryotic-selective aminoglycoside. The synthesis of 6'-F sisomicin is shown in Scheme 1.

Results

Overviews of the bacterial and protozoal cytoplasmic A-site structures in complex with 6'-F sisomicin

Crystal structures of 6'-F sisomicin bound to the bacterial and protozoal cytoplasmic rRNA A-sites, labeled "BACT/F-sisomicin" and "PROTO/F-

sisomicin” (Table 1), respectively, were obtained using A-site RNA models used in our previous studies (Figure 4).^[4-15] In BACT/F-sisomicin and PROTO/F-sisomicin crystals, the asymmetric unit consisted of one and one-half palindromic RNA duplex containing two A-site internal loops, respectively.

In the case of the BACT/F-sisomicin complex (Figure 4, left), only one of the two A-site internal loops in the palindromic RNA duplex was fully resolved, owing to disordered electronic density assigned to the A1492 and A1493 nucleobases that bulge out of the helix (Supplementary Figure 1). 6'-F Sisomicin was observed occupying only the well-defined A-site internal loop mimicking the “on” state of the A-site helix with fully bulged-out A1492 and A1493. However, 6'-F sisomicin was not observed in the second identical binding pocket.

In the case of the PROTO/F-sisomicin crystal (Figure 4, right), we observed the two protozoal A-site internal loops were occupied by 6'-F sisomicin bound within the helix and fixing the A-site in the “on” state with nucleobases A1492 and A1493 bulging out. Binding mode of 6'-F sisomicin within the A-site helices is almost identical with those of other 4,5-disubstituted aminoglycosides.^[29,30]

Binding pose of 6'-F sisomicin within the bacterial A-site

6'-F Sisomicin interacts with the bacterial A-site through eight canonical hydrogen bonds, two bifurcated hydrogen bonds and one C-H...O interaction (Figure 5a). Similarly to the X-ray co-crystal structures for the

parent sisomicin and 6'-OH sisomicin (Supplementary Figure 2 and 3),^[6,21] the unsaturated ring I of 6'-F sisomicin stacks on top of the nucleobase G1491 making a π - π interaction. However, unlike other analogs, the ring I of 6'-F sisomicin forms a different type of pseudo base-pair with A1408 *only through bifurcated hydrogen bonds*, F6'...H-N6_{A1408} and O5'...H-N6_{A1408} (Figure 5a). Therefore, the 6'-F atom behaves as an acceptor of a hydrogen bond, causing a shift in the register of the pseudo base-pair. In the cases of sisomicin and 6'-OH sisomicin, the respective 6'-NH₃⁺ and 6'-OH functional groups of ring I behave as hydrogen-bond donors to the N1 atom of A1408. (Figure 3) Aminoglycosides having a hydrogen bond donor in the 6' position of ring I are known to form pseudo base-pairs with A1408 through two hydrogen bonds, O5'...H-N6_{A1408} and N6'/O6'-H...N1_{A1408} which are required to place ring I in the optimal position for a stacking interaction with the nucleobase G1491 (Figure 5 and Supplementary Figures 2). Ring II of 6'-F sisomicin makes direct interactions with the bacterial A-site through four hydrogen bonds, N3-H...N7_{G1494}, N3-H...OP2_{G1494}, N3-H...OP1_{A1493} and N1-H...O4_{U1495}. Ring III forms four hydrogen bonds to the A-site, O2''-H...O6_{G1405}, N3''-H...N7_{G1405}, N3''-H...OP2_{G1405} and O4''-H...OP2_{U1406}. The aforementioned interactions observed for rings II and III of 6'-F sisomicin are conserved in X-ray co-crystal structures of the parent sisomicin and its 6'-OH derivative in the bacterial A-site (Figure 5a and Supplementary Figure 2).

Binding pose of 6'-F sisomicin within the protozoal cytoplasmic A-site

The palindromic RNA duplex models of the bacterial and eukaryotic A-sites are identical, with the exception of the A1408G substitution. Therefore, almost all interactions observed between 6'-F sisomicin within the bacterial A-site are conserved in the PROTO/F-sisomicin complex (Figure 5). The major difference is found in the geometry of the pseudo base-pair between ring I and nucleobase G1408 that characterizes the protozoal cytoplasmic ribosome. In this case, ring I forms a pseudo base-pair with G1408 through two hydrogen bonds and one C-H...O interaction, F6'...H-N2_{G1408}, O5'...H-N1_{G1408} and C1'-H...O6_{G1408} (Figure 5b). Therefore, the 6'-F atom behaves as the acceptor of a hydrogen bond in the protozoal cytoplasmic rRNA A-site. Importantly, this pseudo base-pair geometry is essentially identical to that observed in 6'-OH sisomicin bound to the protozoal cytoplasmic A-site, where 6'-OH behaves as the acceptor of hydrogen bond and makes a O6'...H-N2_{G1408} hydrogen bond (Figure 3 and Supplementary Figure 4). On the other hand, ring I of sisomicin with a 6'-NH₃⁺ is less likely to participate in a pseudo base-pair with G1408, since the NH₃⁺ group can only behave as the donor of a hydrogen bond (Figure 3). Indeed, our laboratory has made numerous attempts to assemble co-crystals of sisomicin with the eukaryotic A-site RNA model, which to this date have proven unsuccessful or have led to unoccupied A-site RNAs.

Inhibitory activities of sisomicin and 6'-F sisomicin against prokaryotes and eukaryotes

The inhibitory activities of the parent sisomicin and 6'-F sisomicin against pathogenic bacterial species (MIC) and pathogenic protozoal species (EC₅₀) are summarized in Table 2. Validating our hypothesis, 6'-F sisomicin exhibited antiprotozoal activity comparable to the natural aminoglycoside paromomycin, but it was devoid of antibacterial or bacteriostatic activity relative to sisomicin in prokaryotic assays (MICs > 1.0 µg/mL). As expected, the parent sisomicin displayed good Gram-negative or Gram-positive bacteria (MIC values << 1.0 µg/mL). Moreover, there was no evidence of overt toxicity associated with sisomicin or 6'-F sisomicin treatments to the HeLa mammalian cell line. These results should be taken in consideration in the context of our previous observations with 6'-NH₃⁺ and 6'-OH sisomicin analogs,^[13] as well as the structurally matching 6'-NH₃⁺ and 6'-OH neomycin-paromomycin pair of naturally occurring aminoglycosides.^[17] To the best of our knowledge, there are no reports on the antiprotozoal activity of sisomicin. Based upon the computationally modeled structure shown in Figure 3, sisomicin should not be able to form a pseudo base pair with G1408, since the 6'-NH₃⁺ group can only behave as a donor of hydrogen bonds. We were therefore surprised, that sisomicin displayed activity against protozoal species (*Trypanosoma brucei brucei*, *T. brucei rhodesiense*, *T. cruzi* and *Leishmania major*).

Discussion

Based on the crystal structures of 6'-F sisomicin bound to the bacterial and protozoal cytoplasmic A-sites (Figure 5), and the previously reported crystal structure of the parent sisomicin bound to the bacterial ribosome A-site^[6] (Supplementary Figure 2a), we hypothesized that: (i) interactions of 6'-F sisomicin with the bacterial ribosome A-site should be disrupted due its inability to form a stable pseudo base-pair interaction with the A1408 nucleobase. Interestingly, the X-ray co-crystal structure of 6'-F sisomicin in complex with the palindromic RNA duplex comprising two identical bacterial A-sites displays a pose for the 6'-F ring I that was out of register with the highly specific hydrogen-bond and stacking interactions made by numerous aminoglycoside antibiotics (ii) 6'- F-sisomicin should exhibit antiprotozoal activity due to its H-bond acceptor ability with G1408.. (iii) the parent sisomicin should experience ineffective binding to the protozoal cytoplasmic ribosome A-site, since the 6-NH₃⁺ in ring I would act as a hydrogen bond donor and cannot form a pseudo base-pair with the G1408.

We observed that the 6'-F sisomicin possesses moderate antiprotozoal activity (Table 2), which is favorably comparable to the antileishmanial drug paromomycin.^[17] However, contrary to paromomycin or sisomicin, which in agreement with published data, display a strong antibacterial activity,^[22] 6'-F sisomicin does not display any significant antibacterial or bacteriostatic activity, either against laboratory generated *E. coli* and methicillin-sensitive or -resistant *S. aureus* strains (MIC > 1.0 µg/mL, Table 2). Therefore, it can

be concluded that 6'-F sisomicin is not an active antibiotic, and represents a novel example of a eukaryote-selective aminoglycoside.

Contrary to the predictions of the X-ray structural information, sisomicin displays a strong baseline activity as an antiprotozoal, even though its ring I with an 6'-NH₃⁺ group is not likely to form a high-affinity pseudo base-pair with G1408 within the protozoal cytoplasmic ribosome A-site (Figure 3). Indeed, these data suggest that sisomicin with four positively-charged NH₃⁺ groups may have an advantage in cellular uptake and/or may bind to alternative sites besides the protozoal rRNA A-site. These poorly studied interactions should be considered for higher-charge aminoglycosides that could presumably disturb the process of translation and/or ribosomal assembly processes as reported for prokaryotic and eukaryotic full ribosomes.^[31,32] We contend that 6'-F sisomicin is less likely to engage in such unspecific and off-target mechanisms, since the original positively-charged NH₃⁺ group in the parent sisomicin, which is exclusively an H-bond donor, was replaced by a F atom that is exclusively an H-bond acceptor. More broadly, the 6'-fluorine substitution concept to replace a bioactive equivalent hydroxyl compound is easily generalizable and such may prove to be promising for optimization and development of eukaryote-selective antiprotozoal treatments.

Conclusions

We have successfully developed a protozoal-selective aminoglycoside exemplified by 6'-F sisomicin relying on a structure-based design approach inspired by X-ray crystallographic data. We have confirmed that 6'-F sisomicin is effective against pathogenic protozoal species, but largely ineffective as an antimicrobial compound against Gram-negative and Gram-positive bacterial species. To the best of our knowledge, 6'-F sisomicin is the first semisynthetic aminoglycoside displaying such a stark reversal of selectivity between eukaryote and prokaryote species.^[46] The present study expands the scope of small-molecule drugs targeting the eukaryotic ribosomal A-site and demonstrates the usefulness of fluorine as a design element to specifically control hydrogen-bonding interactions of ligands with functional RNA biomedical targets.

Experimental section

6'-Fluoro-sisomicin

Following the procedure reported by Hanessian *et al* (Scheme 1),^[23] sisomicin sulfate (**1**) was converted to 1,3,2',6'-tetraazido-3''-N-Fmoc-sisomicin (**2**), and treated under optimized selenium dioxide allylic oxidation conditions to yield 6'-aldehyde-1,3,2'-triazido-3''-N-Fmoc sisomicin (**3**). The 6'-aldehyde intermediate was subsequently reduced to afford 6'-hydroxy-1,3,2'-triazido-3''-N-Fmoc sisomicin (**4**) using sodium borohydride in THF/MeOH as previously reported.^[13] A solution of the above compound (41.2 mg, 0.055 mmol) in CH₂Cl₂ (100 mL) was treated with KF (6.4 mg, 0.11 mmol) followed by a solution of Phenofluor® (0.1 M in toluene, 1.1 mL), and then treated with of *N,N*-diisopropylethylamine (DIPEA, 17.4 μL, 0.11 mmol). The reaction mixture was stirred overnight at room temperature under an argon atmosphere. The crude mixture was filtered through a Teflon filter and concentrated under reduced pressure. The residue was purified by flash chromatography (2% MeOH in CH₂Cl₂) affording the fluorinated product **5** (23.4 mg, 0.031 mmol, 57%) that was used in the next step without further characterization.

The aforementioned compound **5** (23.4 mg, 0.031 mmol) was dissolved in MeOH (900 μL), and treated with piperidine (32 μL, 0.33 mmol), a solution of PMe₃ (1.0 M in THF, 495 μL, 496 mmol) and NH₄OH (conc., 100 μL) added sequentially, and the reaction mixture stirred at room temperature overnight. The mixture was concentrated under reduced pressure and the residue dissolved in a minimum amount of water. The crude

mixture was loaded to an ion exchange column containing Amberlite® IRC50 (1 mL) and eluted sequentially with water (15 mL), 0.1 N aqueous NH₄OH (18 mL) and 0.3 N aqueous NH₄OH (30 mL). The tubes containing the desired product were combined, concentrated to a minimum volume under reduced pressure and lyophilized affording the title compound as the free base (7.5 mg, 0.0167 mmol of a glassy solid). The product thus obtained was dissolved in an aqueous solution of (NH₄)₂SO₄ (100 µl, 44 mg (NH₄)₂SO₄/mL water, 2 equiv.) and stirred 5 minutes. The mixture was lyophilized overnight affording 6'-F sisomicin sulfate (**6**) as an amorphous solid (8.9 mg, 0.014 mmol, 45%, 26% two steps).

¹H NMR (500 MHz, D₂O) δ 5.63 (d, *J* = 2.0 Hz, H-1'), 5.31 (dt, *J* = 5.4, 3.8 Hz, H-4'), 5.14 (d, *J* = 3.7 Hz, H-1''), 3.96 (d, *J* = 47.5 Hz, H-6'b), 3.94 (d, *J* = 47.5 Hz, H-6'a), 4.23 (dd, *J* = 10.9, 3.7 Hz, H-2''), 4.03 (d, *J* = 12.9 Hz, H-5''b), 4.00 (dd, *J* = 10.4, 8.8 Hz, H-5), 3.86 (td, *J* = 6.5, 2.1 Hz, H-2'), 3.78-3.83 (m, H-4 and H-5), 3.61-3.52 (m, H-3 and H-1), 3.50 (d, *J* = 13.4 Hz, H-5''a), 3.50 (d, *J* = 10.7 Hz, H-3''), 2.93 (s, 3H, C-Me), 2.64 (m, H-3'b), 2.58 (dt, *J* = 12.6, 4.3 Hz, H-2b), 2.41 (dddd, *J* = 17.7, 10.0, 6.8, 3.6 Hz, H-3'a), 1.95 (q, *J* = 12.6 Hz, H-2a), 1.35 (s, 3H, N-Me); ¹³C NMR (126 MHz, D₂O) δ 145.5 (d, ²*J*_{5',F} = 14.5 Hz, C-5'), 101.2 (C-1''), 96.7 (C-1'), 83.4 (C-6), 82.0 (d, ¹*J*_{6'a,F} = 160.1 Hz), 79.8 (C-5), 73.5 (C-4), 70.0 (C-4''), 67.8 (C-3''), 66.4 (C-2'), 63.4 (C-5''), 49.9 and 48.3 (C-1 and C-3), 46.1 (C-2'), 34.6 (N-Me), 27.6 (C-2), 22.1 (C-3'), 21.0 (C-Me); ¹⁹F NMR (471 MHz, D₂O) δ -213.38 (tddd, *J* = 47.5, 10.0, 8.6, 5.4 Hz); HRMS (ESI-TOF) *m/z*

[M + H]⁺ Calc. for C₁₉H₃₆FN₄O₇ 451.25625, observed 451.25632, m/z [M + K]⁺ Calc. for C₁₉H₃₅FKN₄O₇ 489.21214, observed 489.21214.

Crystallizations, Data Collections and Structure Determinations

For the present crystallographic studies, RNA duplexes containing two A-site internal loops were designed (Figure 4). These RNA oligomers were synthesized by GeneDesign, Inc. (Osaka, Japan), purified by 20% denaturing polyacrylamide gel electrophoresis and desalted by reversed-phase chromatography. Single crystals of these RNA duplexes in complex with 6'F sisomicin (BACT/F-sisomicin and PROTO/F-sisomicin, respectively) were obtained in conditions summarized in Table 3. Fresh crystals were mounted in nylon cryoloops (Hampton Research) with the crystallization droplet containing 40% (v/v) 2-methyl-2,4-pentanediol as a cryoprotectant and stored in liquid nitrogen prior to X-ray experiment. X-ray data were collected at the NW-12A and BL-17A beamlines in the Photon Factory (Tsukuba, Japan). These datasets were processed with the program *XDS*.^[33] These obtained intensity data were further converted to structure-factor amplitudes using *TRUNCATE* from the *CCP4* suite.^[34] The statistics of data collection and the crystal data are summarized in Table 1. The initial phases of both the BACT/F-sisomicin and PROTO/F-sisomicin crystals were determined by the molecular replacement method with the program *AutoMR* from the *Phenix* suite^[35,36] The molecular structures were constructed and manipulated with the program *Coot*.^[37,38] The atomic parameters were refined with the program *phenix.refine* from the *Phenix* suite^[35,39] through a

combination of simulated-annealing, crystallographic conjugate gradient minimization refinements and *B*-factor refinement. The statistics of structure refinements are summarized in Table 1. The atomic coordinates of the BACT/F-sisomicin and PROTO/F-sisomicin complexes were deposited to the Protein Data Bank (PDB) with ID codes 5Z1H and 5Z1I, respectively.

Cell culture and Cytotoxicity assays

The determination of the EC₅₀ of the compounds using Alamar Blue was completed as previously described.^[40,41] Briefly, DMSO solutions of the compounds were added to the media and a two-fold serial dilution done across a 96-well plate in quadruplicate (12-point serial dilution). Cells were counted using a CASY Cell Counter and seeded at cell densities given below. After 3 days, 10 mL Alamar Blue (12.5 mg resazurin salt in 100 mL PBS) was added to all wells and incubated for a further 6-8 h. Cell viability was quantified using an FLx 800 plate reader (BioTek) with excitation wavelength 540/35 nm and emission wavelength at 590/10 nm using Gen5 Reader Control 2.0 Software (BioTek). EC₅₀ values were determined using a 4-parameter logistic regression equation using GraFit 5.0 (Erithacus Software).

Bloodstream-form *T. brucei brucei* strain 427 and were grown in HMI-9 media supplemented with 10% foetal bovine serum and 2.5 µg/mL G418 at 37 °C with 5% v/v CO₂ and seeded at 1 × 10³ cells/well. *T. brucei rhodesiense* (strain Z310) were cultured in a similar manner, but in the absence of G418.

HeLa cells (ATCC® CCL-2) were cultured in Dulbecco's Modified Eagle Medium supplemented with 10% foetal bovine serum and grown at 37°C in 5% CO₂ atmosphere and seeded at 1 × 10³ cells per well.

Mid-log promastigote *L. major* MHOM/IL/80/Friedlin were grown at 28°C in M199 media (pH 7.4), supplemented with 40 mM HEPES pH 7.4, 100 µM adenosine, 5 µg/mL haemin and 10% heat-inactivated foetal bovine serum and seeded at 2 × 10⁵ cells per well.

Mid-log epimastigote *Trypanosoma cruzi* CL Brener strain were grown at 28°C in RPMI 1640 medium supplemented with 20 mM HEPES (pH 7.2), 4.9 mg/mL tryptone, 2 mM sodium glutamate, 2 mM sodium pyruvate, 100 µg/mL streptomycin and 100 U/mL penicillin, 20 µg/mL haemin and 10% heat-inactivated foetal bovine serum and seeded at 5 × 10⁵ cells per well.

***Plasmodium falciparum* growth inhibition assays**

P. falciparum 3D7 (obtained from MR4-ATCC) parasites were cultured with human erythrocytes (group B; 3-4% hematocrit) in RPMI medium (Sigma) supplemented with 10% AB⁺ human serum incubated at 37°C in an atmosphere of 92% N₂, 3% O₂, and 5% CO₂ using standard methods.^[42] Synchronized cultures were obtained by 5% sorbitol lysis.^[43] For standard growth inhibition assays, parasitemia was adjusted to 0.5-1% with more than 90% of parasites at the ring stage after sorbitol synchronization. Two hundred microliters of parasite cultures were plated in 96-well plates and incubated for 48 h at 37°C in the presence of the different compounds to be

tested at different concentrations in triplicate. Parasitemia was then determined as described by Aguilera *et al.*,^[44] briefly, fluorescence-assisted cell sorting (FACS). Noninfected RBCs and samples containing parasitized RBCs (including controls without tested compounds) were diluted to a final concentration of 1 to 10×10^6 cells/mL. The cell suspension was stained with SYTO 11 (0.5 mM stock in DMSO, Molecular Probes, Life Technologies) to a final concentration of 0.5 μ M. Samples were analyzed in a BD LSRFortessa cell analyzer (BD; Becton, Dickinson and Company) equipped with a high throughput sampler. Excitation of the sample was done using a 488 nm, air-cooled, argon-ion laser at 15 mW power using forward and side scatter to gate the RBC population, and SYTO 11 green fluorescence (530 nm, FITC filter) was collected in a logarithmic scale. The single-cell population was selected on a forward-side scattergram, and the green fluorescence from this population was analyzed. Parasitemia was expressed as the number of parasitized cells per 100 erythrocytes. Statistical analyses were performed using GraphPad Prism v5.

Antibacterial testing

Compounds were tested against *Escherichia coli* strain DH5 α and *Staphylococcus aureus* strains RN4220 (NCTC8325-4, r⁻ m⁺) and MRSA252 (EMRSA-16) and their potency determined by calculating the minimum inhibitory concentration (MIC) analysis.^[45] Specifically, this was achieved using the microdilution broth method where compounds were serially diluted in microtiter plates with a concentration range from 500 μ M

to 0.24 μM . Each bacterial strain was prepared by inoculation of a colony from an agar plate into 10 ml Müller-Hinton broth and cultured at 37°C with shaking until a turbidity corresponding to a 0.5-McFarland suspension ($\text{OD}_{600\text{nm}} = 0.1$, equivalent to 2×10^7 CFU/mL *S. aureus* and 6×10^7 CFU/mL *E. coli*) was reached. The bacterial inoculum was added to the microtiter plate to give a concentration of 5×10^5 CFU/mL in a final volume of 0.1 mL. Microtiter plates were sealed to prevent desiccation and incubated overnight at 37°C before determination of the MIC value, the lowest concentration of compound that inhibited complete growth of the microorganisms as detected by eye. For further confirmation, the turbidity of each well was accurately measured at 620 nm using a Thermo Scientific Multiskan FC plate reader.

Acknowledgements

This work was supported by Grant-in-Aid for Young Scientists (B) (No. 26860025) and Grant-in-Aid for Scientific Research (C) (No. 17K08248) from the Ministry of Education, Culture, Sports, Science and Technology, Japan (MEXT), and partially supported by the Kurata Grant awarded by the Kurata Memorial Hitachi Science and Technology Foundation, the grant provided by the Ichiro Kanehara Foundation and the Platform for Drug Discovery, Informatics, and Structural Life Science from Japan Agency for Medical Research and Development (AMED). H.K. was supported by the Sasakawa Scientific Research Grant from the Japan Science Society and the

SUNBOR Scholarship. We thank the Photon Factory for provision of synchrotron radiation facilities (Photon Factory Proposal No. 2014G532) and acknowledge the staff of the NW-12A and BL-17A beamlines. We thank our colleague Vu Linh Ly for preparing the hydroxysisomicin intermediate. The Montreal group thanks NSERC for financial support and a fellowship to J.P.M from the Québec Research Fund: Nature and Technology. The TKS group thanks the Medical Research Council (MR/Mo20118/1) for current financial support.

Keywords: aminoglycoside; antiprotozoal activity; fluorination; structure-based drug design; X-ray analysis

REFERENCES

- [1] For recent reviews, see:(a) D. O. Arya, *Aminoglycoside Antibiotics: From Chemical Biology to Drug Discovery*; John Wiley & Sons, N.J. 2007, ISBN-978-0-471-74302-6; (b). B. Becker, M. A. Cooper, *ACS Chem. Biol.* **2013**, *8*, 105-115.
- [2] J. L. Houghton, K. D. Green, *ChemBioChem.* **2010**, *11*, 880-902
- [3] (a) J. M. Ogle, A. P. Carter, V. Ramakrishnan, *Trends Biochem. Sci.*, **2003**, *28*, 259-266; (b) N. Gaerreau de Loubresse, I. Prokhorova, W. Holtkamp, M. V. Rodnina, G. Yusupova, M. Yusupov, *Nature*, **2014**, *513*, 517-522.
- [4] Q. Vicens, E. Westhof. *Structure*, **2001**, *9*, 647-658.
- [5] Q. Vicens, E. Westhof, *J. Mol. Biol.* **2003**, *326*, 1175-1188.
- [6] J. Kondo, M. Koganei, T. Kasahara, *ACS Med. Chem. Lett.*, **2012**, *3*, 741-744.
- [7] B. François, J. Szychowski, S. S. Adhikari, K. Pachamuthu, E. E. Swayze, R. H. Griffey, M. T. Migawa, E. Westhof, S. Hanessian *Angew. Chem. Int. Ed. Engl.*, **2004**, *43*, 6735-6738.
- [8] S. Hanessian, J. Szychowski, S. S. Adhikari, G. Vasquez, P. Kandasamy, E. E. Swayze, M. T. Migawa, R. Ranken, B. François, J. Wirmer-Bartoschek, J. Kondo, E. Westhof, *J. Med. Chem.* **2006**, *50*, 2352-2369.
- [9] J. Kondo, K. Pachamuthu, B. François, J. Szychowski, S. Hanessian, E. Westhof, *ChemMedChem*, **2007**, *2*, 1631-1638.

- [10] S. Hanessian, K. Pachamuthu, J. Szychowski, A. Giguère, E. Swayze, M. T. Migawa, B. François, J. Kondo, E. Westhof, *Bioorg. Med. Chem. Lett.* **2010**, *20*, 7097-7101.
- [11] J. Szychowski, J. Kondo, O. Zahr, K. Auclair., E. Westhof, S. Hanessian, J. W. Keillor, *ChemMedChem*, **2011**, *6*, 1961-1966.
- [12] S. Hanessian, O. M. Saavedra, M. A. Vilchis-Reyes., J. P. Maianti, H. Kanazawa, P. Dozzo, R. D. Matias, A. Serio, J. Kondo, *Chem. Sci.* **2014**, *5*, 4621-4632.
- [13] J. P. Maianti, H. Kanazawa, P. Dozzo, R. D. Matias, L. A. Feeney, E. S. Armstrong, D. J. Hildebrandt, T. R. Kane, M. J. Gliedt, A. A. Godtblum, M. S. Linsell, J. B. Aggen, J. Kondo, S. Hanessian, *ACS Chem. Biol.* **2014**, *9*, 2067-2073.
- [14] J. Kondo, *Angew. Chem. Int. Ed. Engl.* **2012**, *51*, 465-468.
- [15] H. Kanazawa, F. Baba, M. Koganei, J. Kondo, *Nucleic Acids Res.* 2017, 12529-12535.
- [16] For reviews see: (a) J. S. Vakulenko, S. Mobashery, *Clin. Microbiol. Rev.* **2003**, *16*, 430-450; (b). S. Magnet, J. S. Blanchard, *Chem.Rev.* **2005**, *105*, 477-498; (c) Garneau-Tsodikova, S.; Labby, K. J. *MedChemComm.* **2016**, *7*, 11-27
- [17] M. Shalev, J. Kondo, D. Kopelyanskiy, C. L. Jaffe, N. Adir, T. Baasov, *Proc. Natl. Acad. Sci.* **2013**, *110*, 13333-13338.
- [18] For a review see: R. N. Davidson, M. den Boer, K. Ritmeijer, *Trans. Royal.Soc. Trop. Med. Hygiene*, **2009**, *103*, 653-660.

- [19] S. Sundar, T. K. Jha, C. P. Thakur, P. K. Sinha, S. K. Bhattacharya, *N. Engl. J. Med.* **2007**, *356*, 2571-2581.
- [20] M. Shalev, H. Rozenberg, B. Smolkin, A. Nasereddin, C. L. Jaffe, N. Adir, T. Baasov, *Nucleic Acids Res.* **2015**, *43*, 8601-8631.
- [21] J. Kondo, M. Koganei, J. P. Maianti, V. L. Ly, S. Hanessian, *ChemMedChem.* **2013**, *8*, 733-739.
- [22] D. H. Davies, A. K. Mallams, M. Counelis, D. Loebenberg, E. L. Moss Jr, J. A. Waitz, *J. Med. Chem.* **1978**, *21*, 189-193.
- [23] S. Hanessian, J. P. Maianti, V. L. Ly, B. Dechenes-Simard, *Chem. Sci.* **2012**, *3*, 249-256.
- [24] M. Howard, R. A. Frizzell, D. M. Bedwell, *Nature Medicine*, **1996**, *2*, 467-469.
- [25] J. Kandasamy, D. Atia-Glikin, E. Shulman, K. Shapira, M. Savit, V. Belakhov, T. Baasov, *J. Med. Chem.*, **2001**, *55*, 10630-10643.
- [26] I. Nudelman, A. Rebibo-Sabbah, M. Cherniavsky, V. Belakhov, M. Hainrichson, F. Chen, J. Schacht, D. S. Pilch, T. Ben-Yosef, T. Baasov, *J. Med. Chem.* **2009**, *52*, 2836-2845
- [27] I. Nudelman, D. Glikin, B. Smolkin, M. Hainrichson, V. Belakhov, T. Baasov, *Bioorg. Med. Chem.*, **2010**, *18*, 3735-3746.
- [28] M. Shalev, J. Kandasamy, N. Skalka, V. Belakhov, R. Rosin-Arbesfeld, T. Baasov, *J. Pharm. Biomed. Anal.*, **2013**, *75*, 33-40.
- [29] B. François, R. J. Russell, J. B. Murray, F. Aboul-ela, B. Masquida, Q. Vicens, E. Westhof, *Nucleic Acids Res.*, **2005**, *33*, 5677-5690.

- [30] J. B. Murray, S. O. Meroueh, R. J. Russell, G. Lentzen, J. Haddad, S. Mobashery, *Chem. Biol.*, **2006**, 13, 129-138.
- [31] M. A. Borovinskaya, R. D. Pai, W. Zhang, B. S. Schuwirth, J. M. Holton, G. Hirokawa, H. Kaji, A. Kaji, J. H. Cate, *Nat. Struct. Mol. Biol.* **2007**, 14, 727-732.
- [32] I. Prokhorova, R. B. Altman, M. Djumagulov, J. P. Shrestha, A. Urzhumtsev, A. Ferguson, C. T. Chang, M. Yusupov, S. C. Blanchard, G. Yusupova, *Proc. Natl. Acad. Sci. USA*, **2017**, 114, E10899-E10908.
- [33] W. Kabsch, *Acta Crystallogr., Sect D: Biol. Crystallogr.*, **2010**, 66, 125-132.
- [34] Collaborative Computational Project, Number 4. *Acta Crystallogr., Sect D: Biol. Crystallogr.*, **1994**, 50, 760-763.
- [35] P. D. Adams, P. V. Afonine, G. Bunkóczi, V. B. Chen, I. W. Davis, N. Echols, J. J. Headd, L. W. Hung, G. J. Kapral, R. W. Grosse-Kunstleve, *Acta Crystallogr., Sect D: Biol. Crystallogr.* **2010**, 66, 213-221.
- [36] A. J. McCoy, R. W. Grosse-Kunstleve, P. D. Adams, M. D. Winn, L. C. Storoni, R. J. Read, *J. Appl. Cryst.* **2007**, 40, 658-674.
- [37] P. Emsley, K. Cowtan, *Acta Crystallogr., Sect D: Biol. Crystallogr.* **2004**, 60, 2126-2132.
- [38] P. Emsley, B. Lohkamp, W. G. Scott, K. Cowtan, *Acta Crystallogr., Sect D: Biol. Crystallogr.* **2010**, 66, 486-501.
- [39] P. V. Afonine, R. W. Grosse-Kunstleve, N. Echols, J. J. Headd, N. W. Moriarty, M. Mustyakimov, T. C. Terwilliger, A. Urzhumtsev, P. H.

- Zwart, P. D. Adams, *Acta Crystallogr., Sect D: Biol. Crystallogr.* **2012**, *68*, 352-367.
- [40] L. Zhou, G. Stewart, E. Rideau, N. J. Westwood, T. K. Smith, *J. Med. Chem.* **2013**, *56*, 796-806.
- [41] G. J. Florence, A.L. Fraser, E. R. Gould, E. F. King, S. K. Menzies, J. C. Morris, M. I. Thomson, L. B. Tulloch, M. K. Zacharova, T. K. Smith, *ChemMedChem.* **2016**, *11*, 1503-1506.
- [42] W. Trager, J. B. Jensen, *Science*, **1976**, *193*, 673-675.
- [43] C. Lambros, J. P. Vanderberg, *Journal of Parasitology*, **1979**, *65*, 418-420.
- [44] L. Serrán-Aguilera, H. Denton, B. Rubio-Ruiz, B. López-Gutiérrez, A. Entrena, L. Izquierdo, T. K. Smith, A. Conejo-García, R. Hurtado-Guerrero, *Scientific reports*, **2016**, *6*, 33189.
- [45] G. Bou in: Y. Ji (ed) Methicillin-Resistant *Staphylococcus aureus* (MRSA) Protocols. Methods in Molecular Biology, **2007**, vol. 391. Humana
- [46] World Health Organization (WHO), Geneva Switzerland *Working to overcome the global impact of neglected tropical diseases: First WHO report on neglected tropical diseases.* **2010**

Table 1. Crystal data and statistics of data collections and structure refinements.

	BACT/F-sisomicin	PROTO/F-sisomicin
PDB-ID	5Z1H	5Z1I
Crystal data		
Space group	$P2_1$	$I422$
Unit cell (Å, °)	$a = 42.9, b = 31.7, c = 46.7, \beta = 94.8$	$a = b = 46.2, c = 115.3$
Z ^a	1	0.5
Data collection		
Beamline	NW-12A of PF	BL-17A of PF
Wavelength (Å)	1.0	0.98
Resolution (Å)	42.8-2.4	42.9-1.9
of the outer shell (Å)	2.5-2.4	2.0-1.9
Unique reflections	5052	5236
Completeness (%)	99.7	99.8
in the outer shell (%)	100.0	99.2
R_{merge}^b (%)	8.4	7.2
in the outer shell (%)	27.2	27.5
Redundancy	3.5	12.0
in the outer shell	3.6	11.4
Wilson B-factor	39.4	20.7
Structure refinement		
Resolution range (Å)	42.8-2.4	42.9-1.9
Used reflections	5052	5223
R-factor ^c (%)	21.3	19.2
R_{free}^d (%)	26.3	21.1
Number of RNA atoms	893	451
Number of ligand atoms	31	31
Number of water	87	73
Average B-factor	41.2	25.5
of RNA atoms	41.9	24.7
of ligand atoms	26.8	20.1
of water	38.6	32.4
R.m.s.d. bond length (Å)	0.007	0.006
R.m.s.d. bond angles (°)	1.0	1.0

^a Number of RNA duplex in the asymmetric unit.

^b $R_{\text{merge}} = 100 \times \sum_{hklj} |I_{hklj} - \langle I_{hklj} \rangle| / \sum_{hklj} \langle I_{hklj} \rangle$.

^c R-factor = $100 \times \sum ||F_o| - |F_c|| / \sum |F_o|$, where $|F_o|$ and $|F_c|$ are optimally scaled observed and calculated structure factor amplitudes, respectively.

^d Calculated using a random set containing 10% of observations.

Table 2. Inhibitory activities of the parent sisomicin and 6'-F sisomicin against prokaryote (MIC) and eukaryote (EC₅₀)



	sisomicin	6'-F sisomicin
(Bacteria)		
<i>E. coli</i> DH5α	0.14 μg/mL	N.S. ^c
<i>S. aureus</i> RN4220 ^a	0.56 μg/mL	N.S. ^c
<i>S. aureus</i> MRSA252 (EMRSA-16) ^b	0.56 μg/mL	N.S. ^c
(Protozoa)		
<i>T. brucei. brucei</i>	4.34 ± 0.27 μM	18.92 ± 0.61 μM
<i>T. brucei. rhod.</i>	3.92 ± 0.17 μM	17.74 ± 0.82 μM
<i>T. cruzi</i>	3.28 ± 0.18 μM	10.95 ± 0.44 μM
<i>L. major</i>	2.02 ± 0.17 μM	20.14 ± 1.3 μM
<i>P. falciparum</i>	-	> 25 μM
(Mammals)		
Mammalian HeLa	> 500 μM	~400 μM

^a *S. aureus* RN4220 – A methicillin sensitive laboratory strain of NCTC8325, a clinical isolate from 1960).

^b *S. aureus* MRSA252 (EMRSA-16) – A-methicillin resistant pathogenic hospital-acquired strain (clonal complex 30 isolated in 1997)

^c N.S. No MIC values of significance were obtained by testing the bacterial strains with 6'-F sisomicin (> 1.0 μg/mL)

Table 3. Crystallization conditions.

Crystal code	BACT/F-sisomicin	PROTO/F-sisomicin
Temperature	293 K	293K
<u>Sample solution (1 μl)</u>		
RNA	1 mM	1 mM
6'-F sisomicin	2 mM	2 mM
Sodium cacodylate (pH = 7.0)	50 mM	50 mM
<u>Crystallization solution (1 μl)</u>		
Sodium cacodylate (pH = 7.0)	50 mM	50 mM
Spermine tetrahydrochloride	1 mM	1 mM
Lithium chloride	10 mM	100 mM
2-Methyl-2,4-pentanediol	1%	1%
<u>Reservoir solution (250 μl)</u>		
2-Methyl-2,4-pentanediol	40%	40%
Crystals		

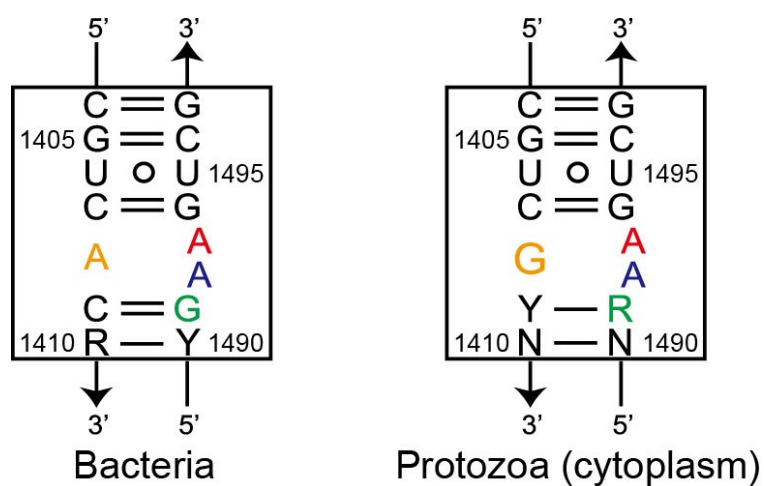


Figure 1. Secondary structures of the bacterial and protozoal cytoplasmic A-sites (R = A or G, Y = C or U, N-N = Watson-Crick base pair). The rRNA nucleobases are numbered according to the numbering used in *E. coli* 16S rRNA. The A/G1408, G/R1491, A1492 and A1493 nucleobases are colored in orange, green, blue and red, respectively.

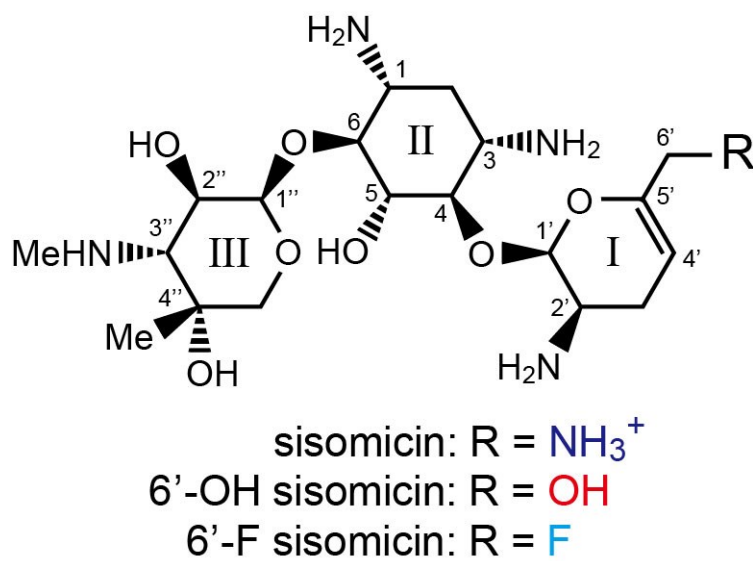


Figure 2. Chemical structures sisomicin, and its derivatives 6'-OH sisomicin^[21] and 6'-F sisomicin.

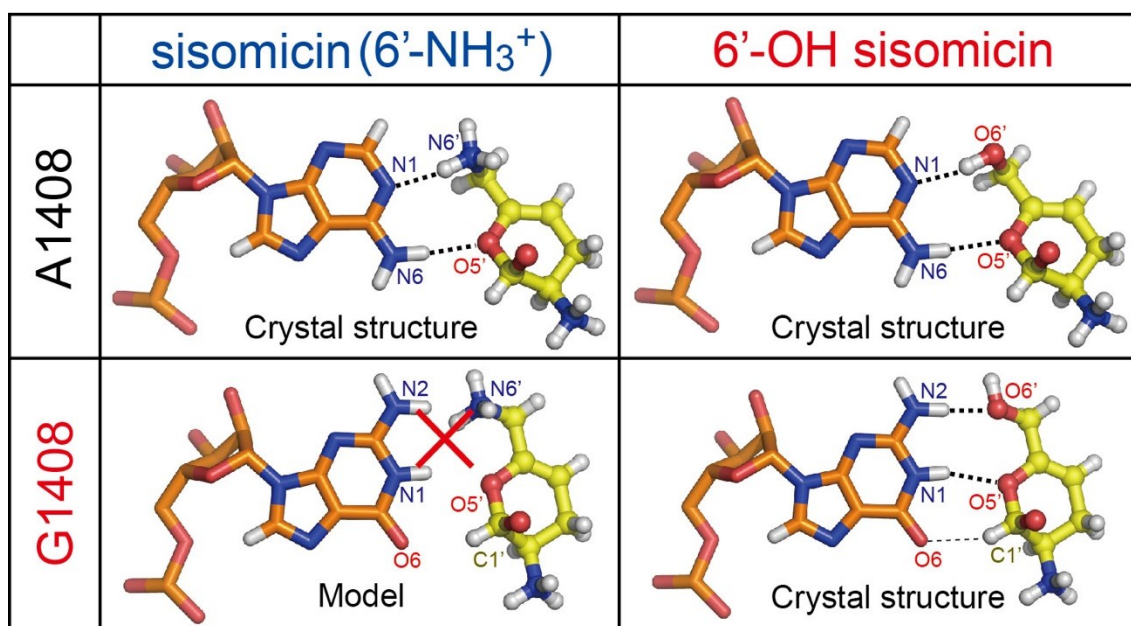


Figure 3. Pseudo base-pairs between the 1408 nucleobase in the prokaryotic (A1408) and eukaryotic cytoplasmic (G1408) A-sites and ring I of sisomicin and 6'-OH sisomicin observed in crystal structures (PDB-ID = 4F8U and 4GPX) or computationally modeled structures. Hydrogen bonds and C-H...O interactions are shown as bold and thin dashed lines, respectively.

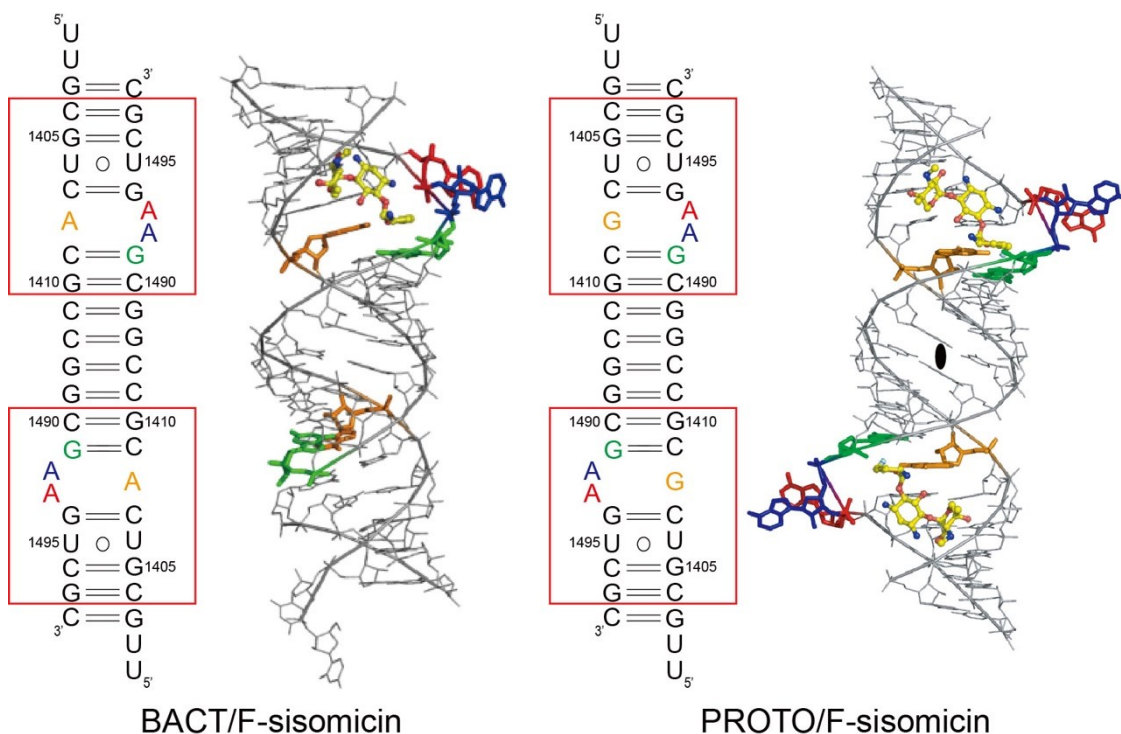


Figure 4. Overall structures of the bacterial and protozoal cytoplasmic A-sites in complex with 6'-F sisomicin (BACT/F-sisomicin and PROTO/F-sisomicin, respectively). A crystallographic two-fold axis located at the center of the PROTO/F-sisomicin crystal is indicated by black oval.

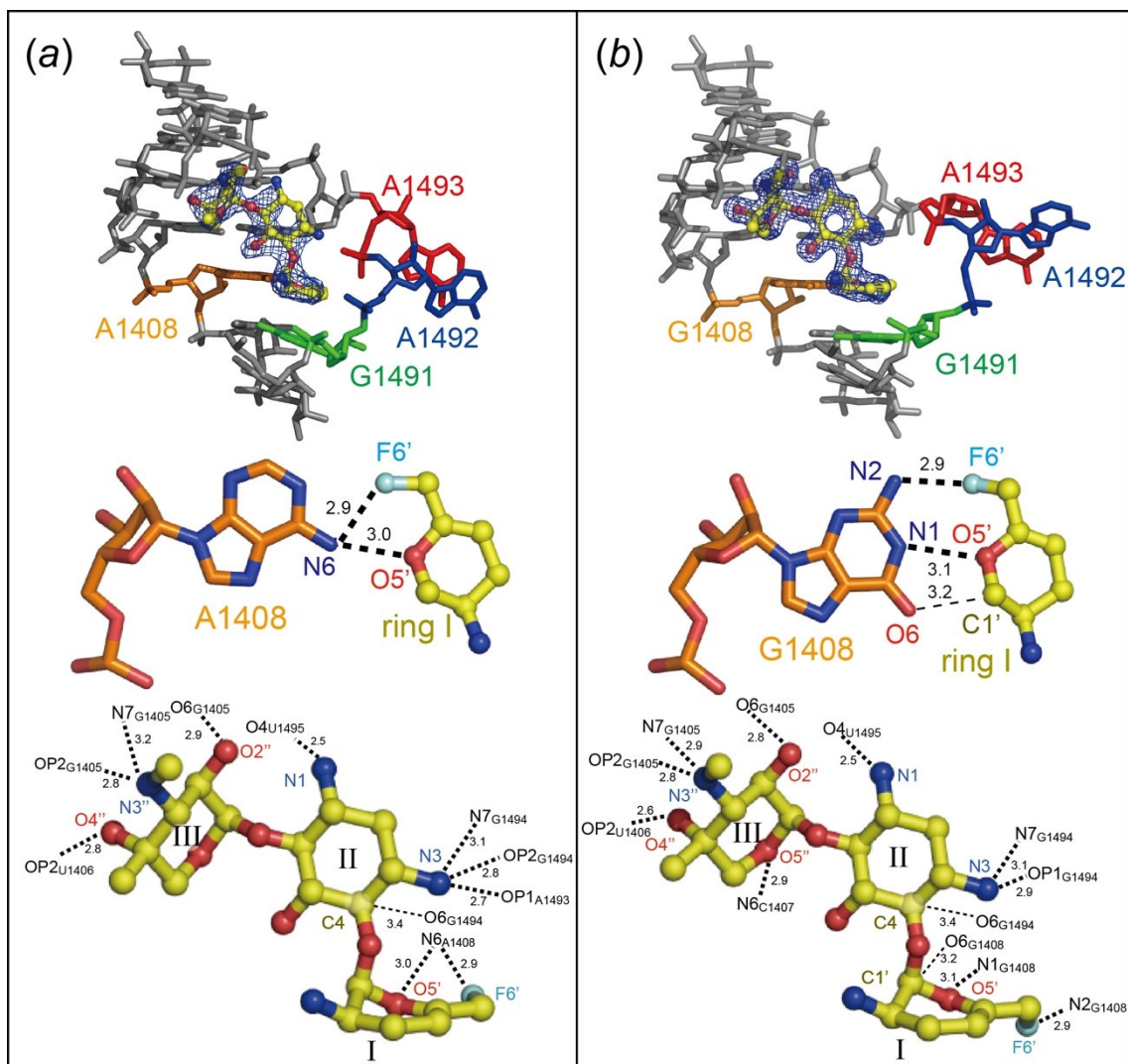
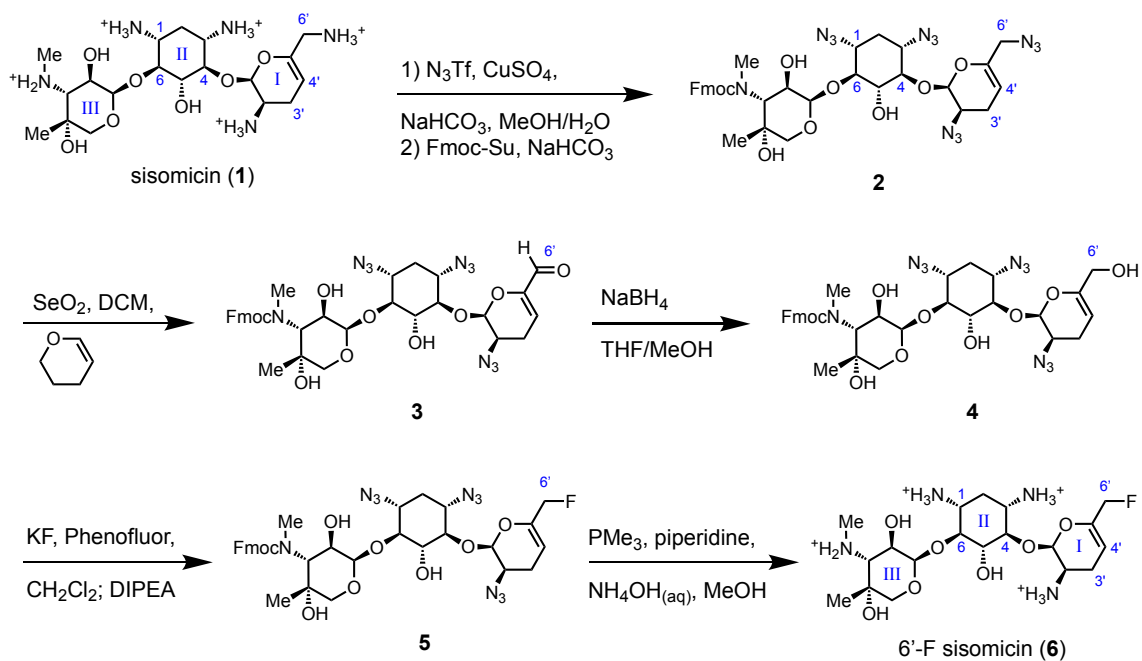


Figure 5. Binding of 6'-F sisomicin to the bacterial and protozoal cytoplasmic A-sites. Overviews (top), pseudo base-pairs between A/G1408 and ring I (middle) and detailed interactions of 6'-F sisomicin to the A-sites (bottom) are shown. The A/G1408, G1491, A1492 and A1493 nucleobases are colored in orange, green, blue and red, respectively. In the top figures, local $|F_o| - |F_c|$ omit maps calculated after removing 6'-F sisomicin are drawn in dark blue at 3 σ contour level. Hydrogen bonds and C-H...O interactions are shown as bold and thin dashed lines with distances in Å, respectively.



Scheme 1. Synthesis of 6'-F sisomicin based on our reported 6'-allylic oxidation^[23] of sisomicin.